# Topic 8: Tomographic Imaging

## 8.1 Introduction

Most generally tomography is the reconstruction of an image from a series of projections, and is most commonly used to image the internal structure of a semi-transparent three-dimensional object, often the human body, as shown in figure 1, where the for three-dimensional object $f(x,y,z)$ we form a *slice* at a given $z$ from a series of projections. From this basic system we can then investigate the total three-dimensional internal structure by taking a series of *slices* as different $z$ as shown in figure 2, which can be combined digitally to for a full three-dimensional representation of $f(x,y,z)$.

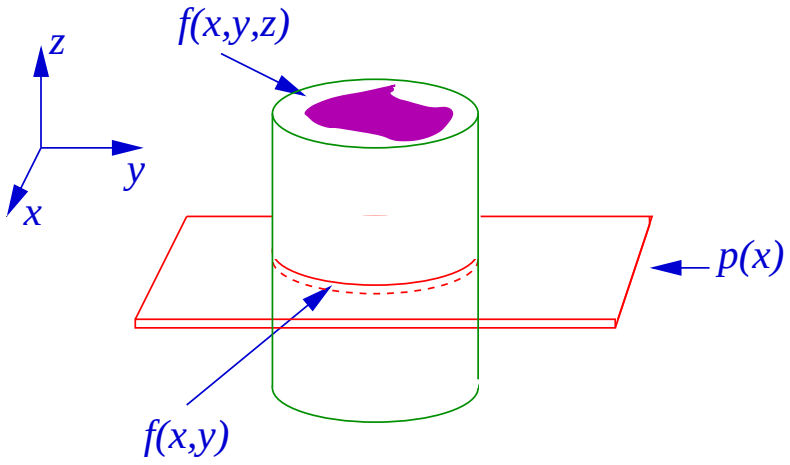


Figure 1: Basic layout of a tomographic system to image a slice through a three-dimensional object.

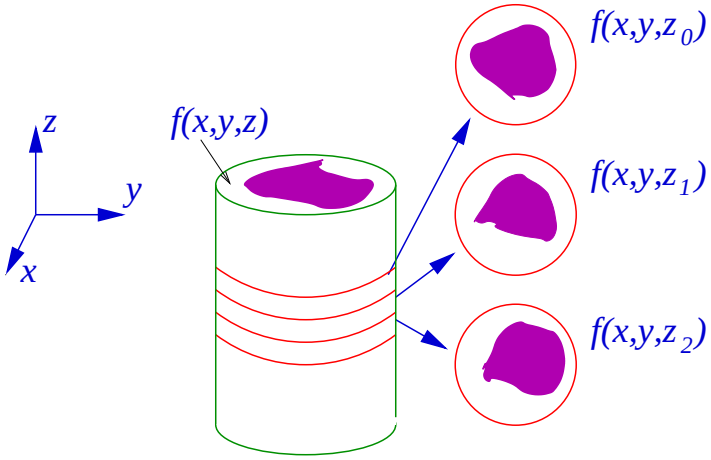


Figure 2: Imaging of a three-dimensional object by taking a series of slices.

This imaging scheme has many applications,

1. *Medical x-ray:* known as *CT-scan*, where X-rays used to form three-dimensional image

of parts of the human body, often of the head/brain as shown in figure 3, but also other part of the body, and even through the main torso.

2. *Geological/Structural x-ray* x-ray analysis of rack samples and fossils either at real size, or at high magnification. Internal analysis of mechanical components, for example crack detection in aero engines.

3. *Astronomical Images:* fan-beam radio astronomy and astronomical interferometry share the same mathematical background.

4. *MRI and PET Medical Imaging:* use the same mathematics of forming images from projections.

Figure 3: CT-scan of a normal brain from http://www.medical.philips.com

In all these applications, the data is not collected as an *image* but is collected as a set on one-dimensional projections from which the image is digitally formed. This reconstructed image is then usually digitally processed and analysed, so in these system digital processing occurs in the image formation and subsequent processing.

## 8.2 Characterisation of System

Basic tomography, and in particular its most common form, X-ray tomography of the human body, is a purely geometric projection scheme where we assume there is no diffraction. In this case this is a very good assumption since the smallest objects of interest are typically $1 \rightarrow 2\,\text{mm}$, while the X-rays have wavelengths of typically 10 nm. Given these assumptions there are two geometries, being

**Collimated Beam :** where the slice being images is illuminated by a thin collimated *sheet* beam as shown in figure 4 and the transmittance is detected by a flat one-dimensional array of detectors.

**Fan beam :** where the slice is illuminates by a thin *fan* being expanding in one-dimension, from a point as shown in figure 5, where the transmittance is detected by an one-dimensional array of detectors forming the arc of a circle.

In both these geometries we form the projection of the transmittance of the slide, and in both cases the problem is to reconstruct $f(x,y)$ from a series of projections taken at a range of angles. The *fan* beam system is the more practical to fabricate and in the the basis of the actual medical

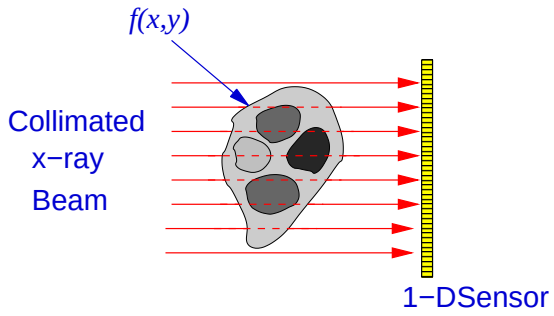


Figure 4: Collimated beam geometry where illuminated X-ray beam is collimated and the detector is a flat one-dimensional array.

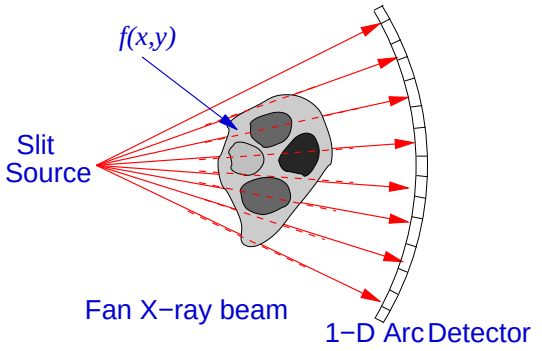


Figure 5: Fan beam geometry where illuminated X-ray beam is in the shape of a fan and the detector is a one-dimensional arc.

systems. However the *collimated* beam is much simpler to analyse and, as we will outline later, the imaging properties of the two are almost identical[1], we will only consider the collimated system in detail.

## 8.3 Collimated Beam Projection

We will consider the case of a *thin* collimated beam of intensity $I_0$ at angle $\theta$ incident on a *three* dimensional object, where the two-dimensional slice in the plane of the beam is given by $f(x,y)$, as shown in figure 6.

If function $f(x,y)$ in the plane of the beam is the x-ray absorption of the object material, then the intensity detected at position $t$ in the detector plane from Ray in direction $s$ is given by,

$$Q_\theta(t) = I_0 \left(1 - \int_{\text{Ray}} f(x,y)\,\mathrm{d}s\right)$$

where $\mathrm{d}s$ is along the direction of the Ray, and $\theta$ is the angle of the beam, from which we can form the normalised absorption of the object being,

$$p_\theta(t) = \int_{\text{Ray}} f(x,y)\,\mathrm{d}s$$

[1] apart from a geometric transformation.

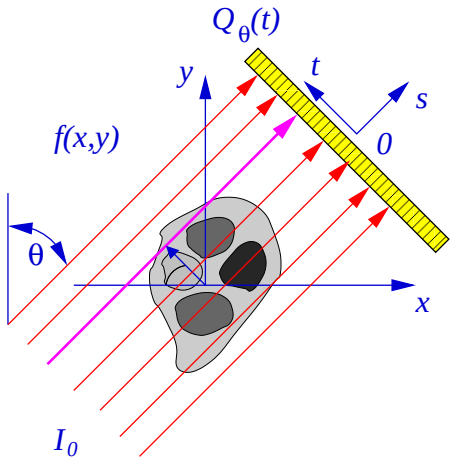


Figure 6: General geometry for collimated beam projection.

Now the ray in direction θ that intersects the detector at position $t$ must have equation,

$$x\cos\theta + y\sin\theta = t$$

A ray, or line, in two dimensions can be represented by a δ-function, being of the form

$$\delta(x\cos\theta + y\sin\theta - t)$$

so being *zero* when not on the line, and integrating to *unity* when on the line. The projection is therefore the object $f(x,y)$, multiplied by the *line* and then integrated, which can be written as a two-dimensional integral given by,

$$p_\theta(t) = \int\!\!\int f(x,y)\,\delta(x\cos\theta + y\sin\theta - t)\,\mathrm{d}x\mathrm{d}y$$

which can then be formed for any θ by, either:

1. Rotating the Object (problem if object is a person!!).
2. Rotating the Detector/Source system.

$p_\theta(t)$ can thus be considered as a *two*-dimensional transform of the data into $\theta, t$ space and is known as that *Radon Transform* of $f(x,y)$ being the fundamental equation in tomographic imaging. Tomographic imaging thus consists of collecting the *Radon Transform* of the slice, and then digitally inverting the this transform to get the slice absorption $f(x,y)$. It is this problem we need to solve.

## 8.4 Fourier Inversion Theorem

First consider the *Radon Transform* in the Fourier domain. Start with the case where $\theta = \frac{\pi}{2}$, so the projection is along the $x$ axis, so we have from the definition of the *Radon Transform* that,

$$p_{\pi/2}(t) = \int\!\!\int f(x,y)\,\delta(y-t)\,\mathrm{d}x\mathrm{d}y$$

which from the shifting property of the δ-function, we have,

$$p_{\pi/2}(t) = \int f(x,t)\,\mathrm{d}x$$

being as expected a projection along the $x$-axis.
We know that the two-dimensional Fourier transform of $f(x,y)$ is

$$F(u,v) = \iint f(x,y)\,\exp\left(-\imath 2\pi(ux+vy)\right)\,\mathrm{d}x\mathrm{d}y$$

so with $u = 0$, we get can write the as,

$$F(0,v) = \int \left[\int f(x,y)\,\mathrm{d}x\right]\,\exp(-\imath 2\pi v y)\,\mathrm{d}y$$

we then the substitute for the [] and with a change of integration variable from $y$ to $t$, we get that,

$$F(0,v) = \int p_{\pi/2}(t)\,\exp(-\imath 2\pi v t)\,\mathrm{d}t$$

which is simply the Fourier Transform of the projection data which is what we measure in the tomographic system. Therefore the Fourier transform of $p_\theta(t)$ gives one *line* in the two-dimensional $F(u,v)$ Fourier space, with for $\theta = \pi/2$ is the *vertical* line with $u = 0$ as shown in figure 7.

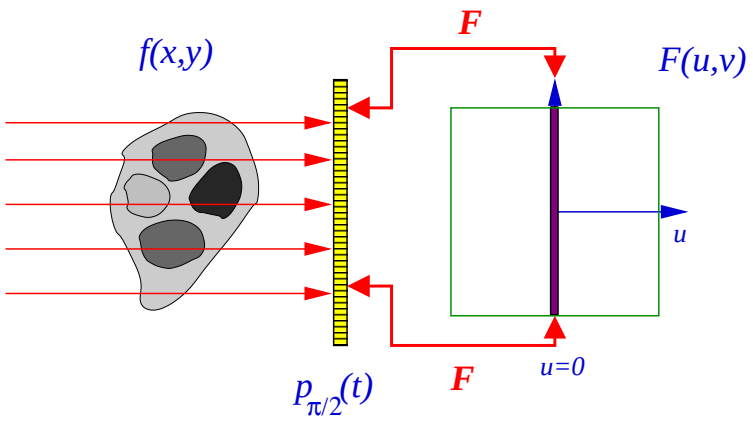


Figure 7: Projection and relation in Fourier space when $\theta = \pi/2$.

If we now define the one-dimensional Fourier of $p_\theta(t)$ at angle θ to be,

$$P_\theta(w) = \int p_\theta(t)\,\exp(\imath 2\pi w t)\,\mathrm{d}t$$

Now consider a projection at angle θ which can be considered taking a projection of a rotated version of the original slice $f(x,y)$, denotes by $f(t,s)$ where

$$\begin{aligned} t &= x\cos\theta + y\sin\theta \\ s &= y\cos\theta - x\sin\theta \end{aligned}$$

so that the detected projection at angle θ is simply given by

$$p_\theta(t) = \int f(t,s)\,\mathrm{d}s$$

which has one-dimensional Fourier transform of

$$P_\theta(w) = \int \left[ \int f(t,s)\,\mathrm{d}s \right] \exp(-\imath 2\pi w t)\,\mathrm{d}t$$

which in $(x,y)$ coordinates, gives,

$$P_\theta(w) = \iint f(x,y)\,\exp\left(-\imath 2\pi w(x\cos\theta + y\sin\theta)\right)\,\mathrm{d}x\mathrm{d}y$$

Similarly we can express the two-dimensional Fourier transform $F(u,v)$ in polar coordinates $w,\theta$ by taking,

$$u = w\cos\theta \quad \text{and} \quad v = w\sin\theta \quad \text{with} \quad w = \sqrt{u^2+v^2}$$

to give function $F(w,\theta)$, which gives is that

$$F(w,\theta) = \iint f(x,y)\,\exp\left(-\imath 2\pi w(x\cos\theta + y\sin\theta)\right)\,\mathrm{d}x\mathrm{d}y$$

so we immediately have that

$$P_\theta(w) = F(w,\theta) = F(u,v)$$

which is the Fourier transform of the slice, $f(x,y)$, which is what we want to measure. Therefore if we measure $p_\theta(t)$, the projection at a range of angle, so forming

$$p_\theta(t) \quad 0 \le \theta \le \pi$$

Then by taking the one-dimensional Fourier transform at each $\theta$, we get $P_\theta(w)$, which we have just shown, is $F(u,v)$, which we can then take the two-dimensional inverse Fourier transform to get the required $f(x,y)$ the absorption slice through the object. This is known as the *Fourier Inversion Theorem*, and is the mathematical foundation[2] of tomographic imaging.

This can also be explained in terms of diagrams, where we have seen in figure 7 that when $\theta = \pi/2$ we get a *vertical* line in the Fourier plane $F(u,v)$, and similarly if we rotate the direction of projection to arbitrary angle $\theta$, then as shown in figure 8, we get another line in Fourier space now at angle $\theta$. Therefore if we take a series of projection for $\theta = 0 \to \pi$, then we can *fill-in*, or sample, $F(u,v)$ over all $u,v$. We can then inverse transform to get the required $f(x,y)$, the absorption of the slice.

## 8.5 Interpolation Problem

The biggest problem with collecting tomographic data is interpolation, since we collect $p_\theta(t)$ at sample intervals of $\Delta t$ and $\Delta\theta$, and so in Fourier space we are effectively sampling on a polar grid as shown in figure 9 with intervals,

$$\Delta w = \frac{1}{N\Delta t} \quad \text{and} \quad \Delta\theta$$

where $N$ is the number of elements in the linear array used to collect $p_\theta(t)$. To take the inverse two-dimensional discrete Fourier transform to form the final image we need sampled $F(k,l)$ data on a regular sampled sampled grid which must be done by interpolation from the $\Delta w, \Delta\theta$ samples.

[2] There are other way to formulate tomographic imaging, but they are actually mathematically equivalent to the Fourier Inversion Theorem.

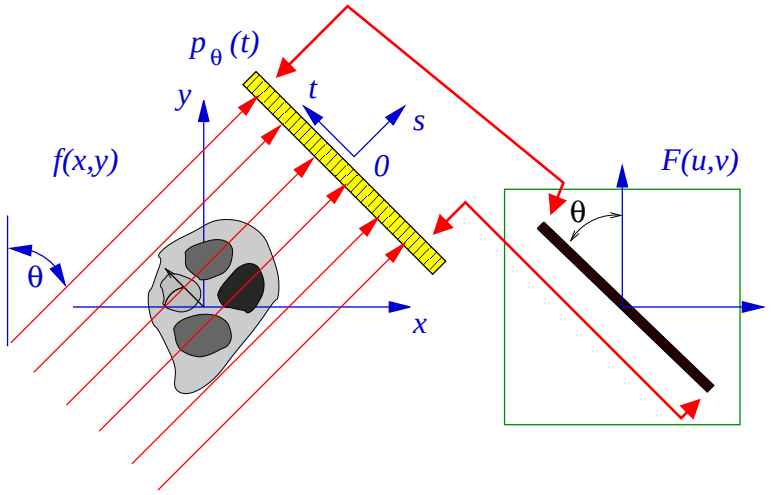


Figure 8: Projection and relation in Fourier space at arbitrary θ.

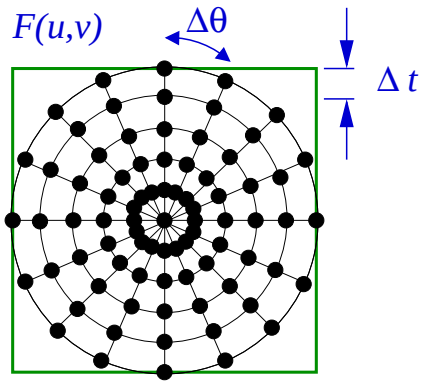


Figure 9: Polar sampling in Fourier space.

This is the major difficult with this interpolation is that while at low spatial frequencies, near the centre of $F(u,v)$ there are many samples, at higher spatial frequencies the $\Delta w, \Delta\theta$ samples are sparcer, which results in undersampling, and hence aliasing at high spatial frequencies. This results in high frequency noise in the reconstrcution, giving for example the straight line patterns in the scan of a sheeps neck in figure 10.(a). In tomographic images, where for speed this inetrpolation is usually either zero-order, being nearest neighbour, or first order being bi-linear interpolation, and while more complex interpolation schemes can help to reduce some of the effects, typically some reconstrcuion artifacts remain.

Since we are filling up the Fourier plane *line-at-at-time* then if we are unable to scan over ther whole $0 \rightarrow \pi$ angular range there will be parts of the Fourier plane than are left undetermined, for example, figure 11 show the Fourier space when only a $0 \rightarrow \pi/2$ angular range has been used. The effect is simular to a Fourier space filter with blanks of the black region of Fourier plane.

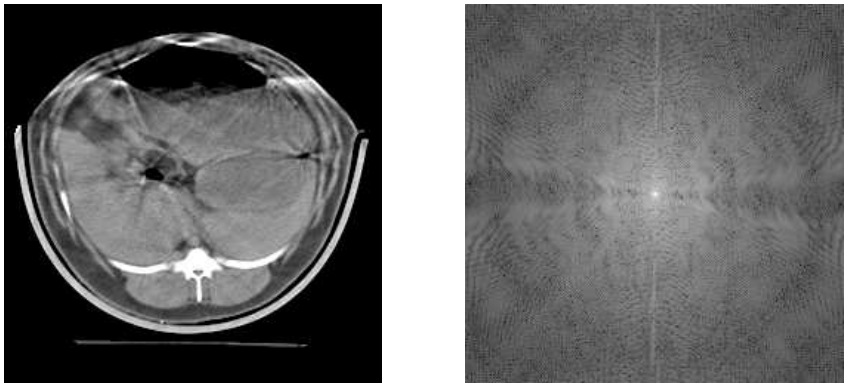

(a) (b)

Figure 10: CT Reconstrcution of a sheeps neck (a) real space reconstrcution, (b) modulus of the Fourier transform.

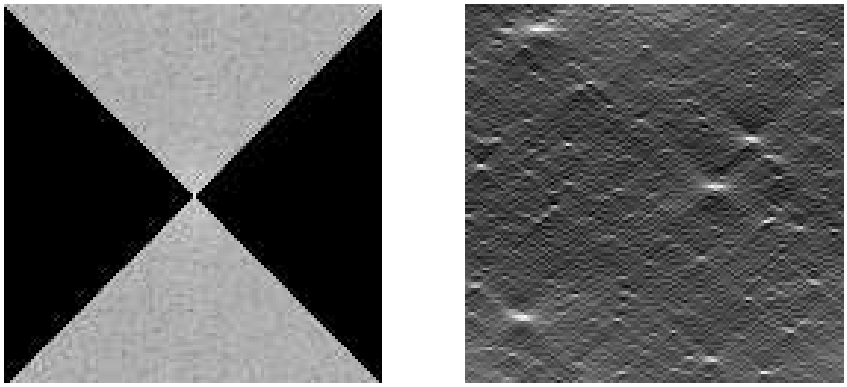

(a) (b)

Figure 11: Effect of limited angle of data collection ins (a) Fourier space, (b) real space reconstruction.

## 8.6 Filtered Back Projection

An equivalent scheme for tomographic reonstruction is *filtered back projection* where the reconstuction is formed by processing the detected projections $p_\theta(t)$ one at a time and *adding* then to the reconstcrution in real space. This scheme has two advanages over the *Fourier Inverseion* scheme above, is that

1. Image is formed is *real time* during the scan so rather than having to wait for all the data to be collected. Therefore faulty scans, for example where the patient moved, can be aborted without subjecting the parient to the full radiation dose.

2. Removes the need for the final , computationally expensive, two-dimensional Fourier transform[3].

Due in particualr to (1), this is the perfered ronstruction algorithum used in medical tomography, it is also the basis for the more complex reconstrcution from the more practical *fan-beam* geometry.

[3]With fast modern computer this has become less of an issue.

If we have

$$f(x,y) = \int_0^{\infty} \int_0^{2\pi} F(w,\theta) \exp(\imath 2\pi w(x\cos\theta + y\sin\theta))\, w\, \mathrm{d}w\mathrm{d}\theta$$

Now if $f(x,y)$ is real, then due to symmetry condition of the FFT, we have that,

$$F(w,\theta+\pi) = F(-w,\theta)$$

we can change the limits of the integration if the inverse transform to get that

$$f(x,y) = \int_{-\infty}^{\infty} \int_0^{\pi} F(w,\theta) \exp(\imath 2\pi w(x\cos\theta + y\sin\theta))\, |w| \mathrm{d}w\, d\theta$$

Now Consider a rotated coordinate system at angle $\theta$, so that

$$t = x\cos\theta + y\sin\theta$$

we get the simpler expression that:

$$f(x,y) = \int_0^{\pi} \left[ \int_{-\infty}^{\infty} P_\theta(w)|w| \exp(\imath 2\pi w t)\, \mathrm{d}w \right] \mathrm{d}\theta$$

where we note from previous that we have that,

$$P_\theta(w) = F(w,\theta) = F(u,v)$$

where $P_\theta(w)$ is the 1-D Fourier Transform of the projection at angle $\theta$. Now define a *filtered* projection of

$$q_\theta(t) = \int_{-\infty}^{\infty} P_\theta(w)|w| \exp(\imath 2\pi w t)\, \mathrm{d}w$$

which, from the Convolution Theorem, we have have that:

$$q_\theta(t) = p_\theta(t) \odot h(t)$$

where $h(t)$ is the filter function

$$h(t) = \mathcal{F}\{|w|\}$$

which is equivalent to High Pass filtering the one-dimensional projection. the final image is given by

$$f(x,y) = \int_0^{\pi} q_\theta(x\cos\theta + y\sin\theta) d\theta$$

**Note :** function $|w|$ is discontinuous as $w = 0$ so $\mathcal{F}\{|w|\}$, in the strict sense, does not exist, however the Digital approximation is calculable.

This scheme is implemented as outlined in figure 12 where for each angle $\theta$ the one-dimensional collected data $p_\theta(t)$ is colvolved with $h(t)$ to forms the *filtred* porjection $q_\theta(t)$. This is then *back-projected* across the reconstruction, so being added to $\hat{f}(x,y)$ at angle $\theta$, so biulting up the image *projection at a time*. In practice this operation is frequently combined with low pass filtering to prevent noise dominating the reconstruction. Mathematics of both reconstruction techniques are identical, and get same problem of non-linear sampling in Fourier space but its computationally simpler simce no final two-dimensional Fourier transform is needeeds for lend it self to *near real-time* use.

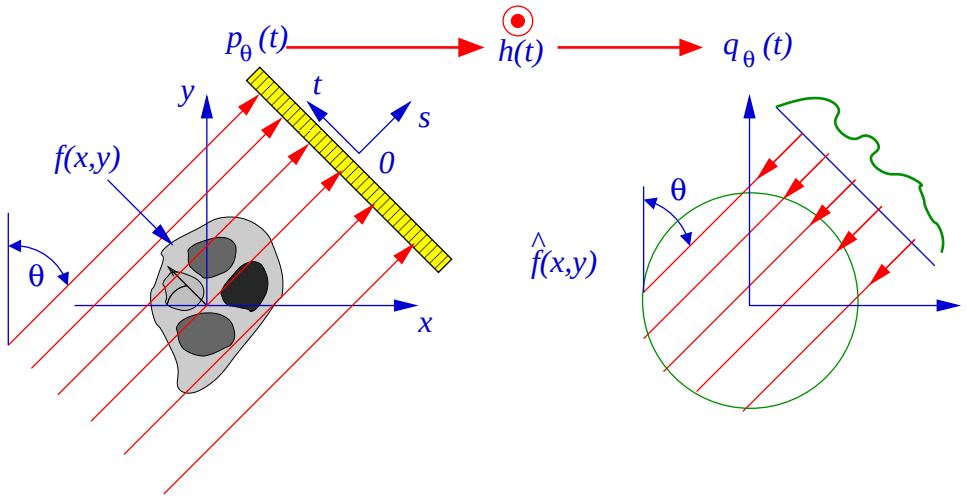


Figure 12: Schamtic layout of filter back-projection.

## 8.7 Typical Images

A typical tomographic result is show in figure 13 showing s section through a human head with an injury on the right side. In such an image the bone is *white* which corresponds to *low absorption* while the water rich tissue of the brain is *high absorption* and is shown up as black. Imaging of the bone is clearly very easy being very high contrast, but the imternal brain strcuture is much lower constrast and is typically image processed, for example median filtered to reduce the noise followed by histogram equalisation to enhance the contrast, before the image is used clinically.

Figure 13: Typical section through a human head showing an injury

If a whole series of scans are taken at different planes as shown in figure 14 (a) & (b) showing a scan twards to the top and middle of the head respectively, then a full three-dimensional reconstrcution of the scull can be formed as shown in figure 14 (c). Here the outline of the *bone* has been extracted from the slices by thresholding, and then the slices aligned digitally to form the three dimensional model which can then be digitally rotated using computer graphics. This type of imaging make extensive use of digital processing both to form each slice, but then also to process each slice to form the final three-dimensional model.

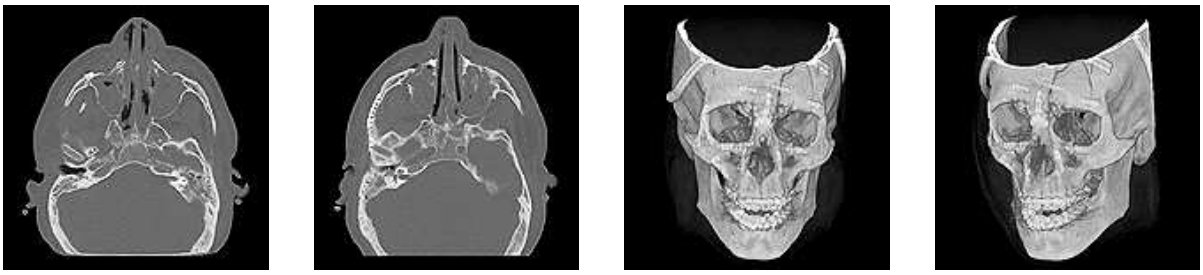

(a) Top (b) Middle (c) Full three dimensional reconstrcution.

Figure 14: Full three-dimensional reconstrcution of the bone struction of a human head, from www.picker.com.

## 8.8 Practical system configurations

To implement *collimated beam* tomography system we ideally need to produce a thin collimated beam beam of x-rays. This is almost impossible to produce since there are no effective or efficient beam shaping lenses that operate in the x-ray region. The only true *collimated beam* is shown in figuge 15 where there is a single x-ray source and detector which make a single intensity measure along a single line. The x-ray source and detector are then scanned at the same speed making a series of measurements at one angle. The x-ray source and detetcor system are then rotatwd about the obejct and the scan repeated. This system is very slow to collect data and is mechanically complex with a two-dimensional scan. More importantly only a tiny fraction of the x-rays are detected and form part of the imaging system; most of the rest being lost in the sample. Such system are not useful for images of live systems where it is essentail to minimise the x-ray dosage, but is used for very dense and absortpive samples such as rocks and fossels which can be subjected to extended x-ray radiation without damage.

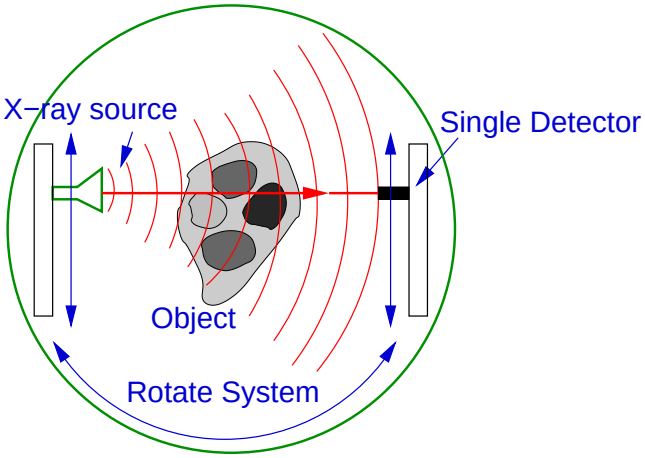


Figure 15: Point-by-point tomographic collection system.

The pratcical system is to illuminate with a *line* source and collect data from a linear array detectors which gives a whole series of ray in parallel in a *fan beam* geometry. There are two viable geometries shown in figure 16, these being *equiangular rays* where the detetcor forms the arc of a circle centred on the source slit. The detected rays are therefore seperated by an equal angle. The alternative geometry is to have a flat detector array, known as *equispaced*

*detectors* where there the ray angular separation now depends on position. All modern tomography systems use *equiangular rays*, with typically, the source and detecor arc rotated about the object.

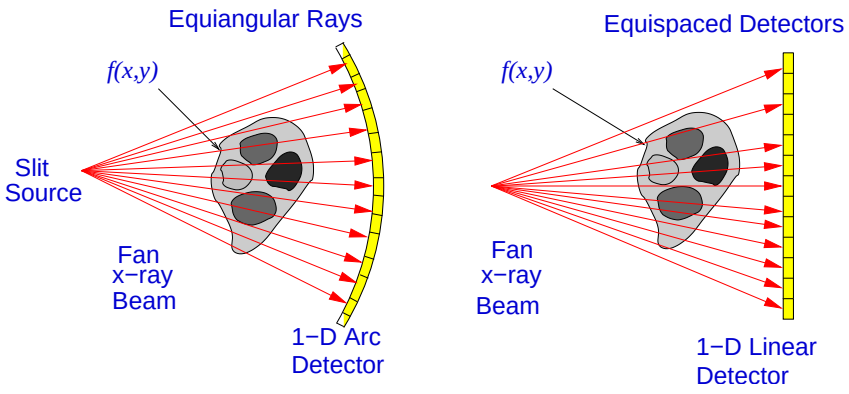


Figure 16: The two fan beam geometries, equiangular rays or equspaced detectors.

A layout of a typical conventional scanning system is shown in figure 17 (a) where the X-ray source and curved detector array are rotated about the object, typically a part of the human body[4]. To for a complete three-dimensional image the subject is then moved, on a translation table, *one slide at a time* through the machine and the scan repeated for each slice. This is a complex mechanical system and is relatively slow, detecting one fan beam projection at a time. The faster *spriral scan* system shown in figure 17 (b) has been recently developed where there is a complete 360° ring of detectors and multiple x-ray sources are rotated inside the ring. Each source is in a diffent plane, so for three sources this system images three *slices* in one rotation. The subject is then moved through the system on a continiously moving table with each scan forming a spiral pattern. This system is much faster, but is also much more expensive due to the need for multiple x-ray sources and a complete detector ring. The data is also in a more complex format so needing greater computer power to process it. Modern sytsem of the spiral format can complete a scan of the human head in about 15 → 30 seconds.

(a) Conventional Scan

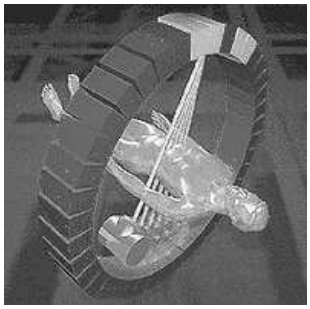

(b) Spiral scan

Figure 17: Scanning geometry used in commercial tomographic scanners, (a) conventional scan and (b) newer high speed sprial scan.

[4]For scanning of inert samples it is easier to rotate the object rather than the source and detector array.

## 8.9 Fan Beam Reconstuction

Tomographic reconstruction in fan beam geometry is conceptually identical to the collimated beam. The geometry of the fan beam system is shown in figure 18. So when the source is rotated by angle $\beta$ with respect to the horizontal then the data collected is

$$r_\beta(\gamma)$$

where $\gamma$ is in the range $-\gamma_M \rightarrow \gamma_M$ being limited by the length of the array. This data can then be collected for a whole range of $\beta$ between $0 \rightarrow 2\pi$.

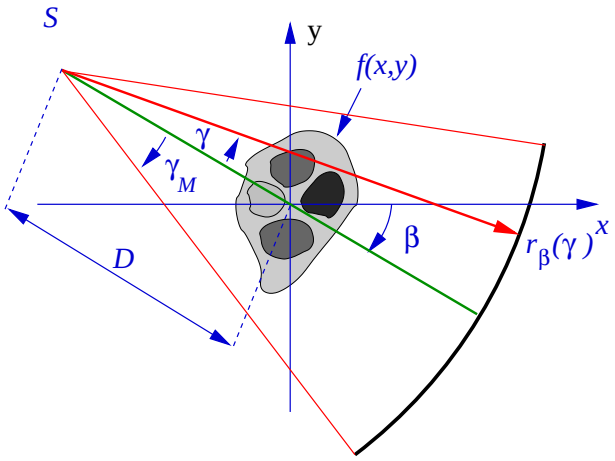


Figure 18: Geometry of the fan beam tomography system.

The reconstrcution can then be implemented by filtered back projection combined with a simple coordinate transformation[5], and the reconstruction becomes, for each projection,

1. Scale the collected $r_\beta(\gamma)$ by $\cos(\gamma)$.
2. Convolve with a one-dimensional filter, to form a filtered version of $r_\beta(\gamma)$, denoted at $s_\beta(\gamma)$.
3. Backproject the data back across the rays of the equiangular fan as shown in figure 19

which is repeated for all angles $\beta$, now in the range $0 \rightarrow 2\pi$ to form reconstruction $\hat{f}(x,y)$. With modern computer system this type of reconstruction is easily performed in *real time* with the scan speed being limited by the movement of the mechanical system. This system shown the aberrations are the collimated beam system, the main problem being interpolation errors which now occur as the filtered $s_\beta(\gamma)$ is backprojected across the reconstruction at a limited range of angles.

The alternative scheme is to collect the projection data $r_\beta(\gamma)$ in the *fan-beam* geometry and then noting that each ray $r_\beta(\gamma)$ is equivalent to a ray $p_\theta(t)$ is the collimated beam geometry with

$$\theta = \beta - \gamma \quad \text{and} \quad t = D\tan\gamma$$

[5]Details of this are beyond this coures.

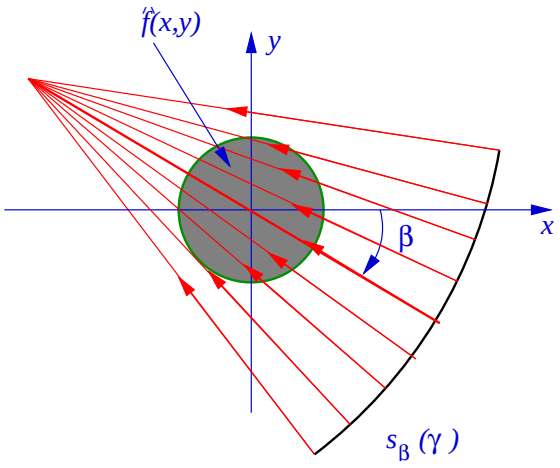


Figure 19: Backprojection in fan beam geometry.

where $D$ is the distance from the slit source to the centre of the object as shown in figure 18. Therefore the projections collected in *fan-beam* geometry can be *ray sorted* to give the equivalent $p_\theta(t)$ projections which can then be reconstrcuted by either the Fourier inversion or collimated back projection scheme. In practice this scheme has exactly the same interpolation errors as the fan-beam back projection and the additional computationally costly sorting of the projection, so in pratcice does not have any advantage, and is actaully more computationally expensive.

There are also a range of other more complex schemes which avoid the Fourier step by forulating the whole reconstruction as a set of coupled linear equaitions that are then solved by minimisation. These schemes are computationally much more expensive and not used routinely in scanner systems but as an alternative scheme when standard filtered backprojection gives unexpected results.

## 8.10 Other Tomographic Imaging Systems

There are a range of other tomographic imaging systems used mainly in medical applications but also in radio astronomy where the reconstrcution from a fan-beam radio telescope is identical to collimated beam projection with the image formed by Fourier inversion. In astronomical radio interferometry, which consists of taking coherent signal from two movable radio telescopes the *image* is also collected in Fourier space but *one spatial frequency at a time* being given by the separation between the telescopes. Again the image is formed by Fourier inversion but now with a very sparcely sampled Fourier space.

The main tomographic systems are used in medical imaging, the two most common being *magnetic resonance imaging* and *positorn emission tomography* which are outlined in the next two sections.

### 8.10.1 Magnetic Resonance Imaging

This system used the nuclear magnetic resonance of protons in hydrogen as an imaging system. The proton spins are aligned with a very large magnetic field, several Tesla, and when then decay they give out small amounts of eletro-magnetic radiation that cen be detetced by exetrnal

coils. This has the effect of measureing local water content[6]. The location of the measuresment is controlled by varying the gradient of the magnetic field, and results on the meausuremants being averaged along line through the object, so its is effectively a tomographic technique using the same reconstrcution scheme as discussed for x-ray computer tomography. Typical MRI images are shown in figure 20 which can be used to give horizontal or vertical scan, which as fro x-ray images, can then be formed into full three-dimensional models by further processing.

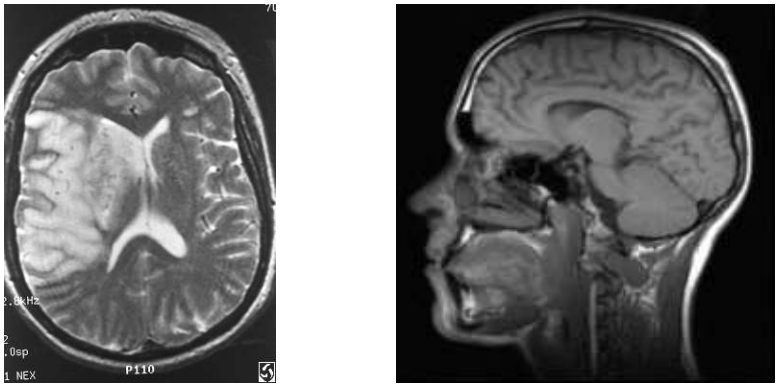


(a) Horizontal Scan (b) Vertical scan

Figure 20: Typical MRI images of the human head, (a) horizontal section, and (b) vertical section.

MRI images shown excellent detail of soft tissue being but rather poor contrast in bone which has a low water content. It is therefore a complementary techniques to x-ray tomography, and is also much *safer* for the patient which no know radiological effect. However the data collection is much slower and the initial cost and running cost of the scanner are many times that of the x-ray system .

### 8.10.2 Positron Emission Tomography

In this system the subject is injected with short lived radio isotope, usually $^{15}O$[7] , which decays by positron emission, which in turn annihilates with alocal electron to give *two* $\gamma$-rays of energy 511 Mev travelling in opposite directions. If the subject is the surrounded by a ring of detectors as shown in figure 21 (a), then a simultaneous detection of a pair of $\gamma$-rays of the correct energy in detectors $A$ and $B$ means that a $e^+ + e^-$ annihilation occured on the line between $A \rightarrow B$. When data is collected for a long period it will thus give the *average* number of annihilations along the line between any two detectors, which is again tomographic data collection. This can then be reconstrcuted to form a slice image as shown in figure 21 (b) shown annihilation activity. In this scheme the oxygen isotope accumulates the in active regions where cell are taking up oxygen, so if applied to the brain, will give a image of *brain activity*. If the system is run in real time it can therefore let you see the *brain thinking*.

This scheme has a number of technical problems, maining the number of annihilations is small, so collected data is severly corrupted by Poisson noise, which results is a rather noise reconstr-cution. The image resolution is also fundamentally limited by the mean free path of the emitted

[6]The decay time are also influenced by their local environment, which allows the imaging system to be tuned to measure different local parameters.

[7]$^{11}C$, $^{13}N$ and $^{18}F$ are also possible but less commonly used.

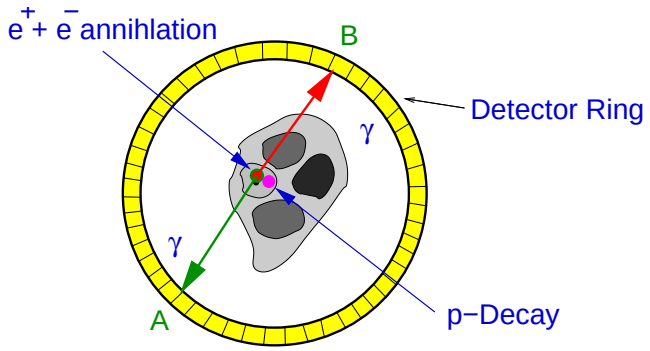


(a) PET system

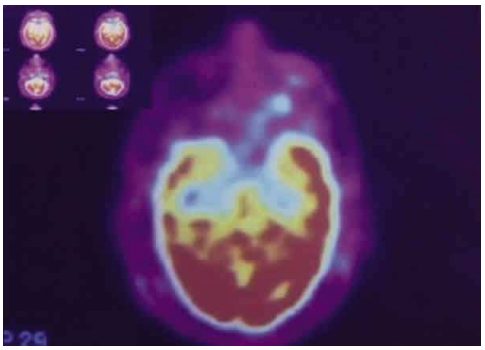

(b) Typical image

Figure 21: Layout and typical image from positron emission tomography (PET) systems.

positron before the $e^+ + e^-$ annihilation occurs. In the brain this is typically $1 \rightarrow 2$ mm, so giving an effective resoluition limit of about 2 mm, being about $\times 10$ poorer that the best modern x-ray or MRI systems.

The other major technical problem is that $^{15}$O does not occur naturally and has a half-life of only 20 minutes. It therefore has to be produced, by borbardment of water in a particle accelerator, injected into the subject and the image taken in typically $20 \rightarrow 30$ minutes. This means a particle accelatator has to located *next door* to the scanner and typically dedicated to the imaging system with $^{15}$O prepared for each scan. This make whole process extremely expensive bot to install and run; it also needs a very large facility to house the particle accelerator. As a result there are only a handful systems, currently four in the UK[8].

# 9 Summary

This section contains a description of tomographic imaging and the basic schemes used to form images.

- Basic concepts of tomographic imaging.
- Collimated beam projection.
- Fourier inversion theorem
- Interpolation problems and issues.
- Filtered back projection for collimated beam reconstruction.
- Pratcical systems and problems.
- Fan beam reconstrcution.
- Other tomographic imaging systems.

[8] as of 2003